Journal of Cardiovascular Translational Research (2024) 17:598–608
https://doi.org/10.1007/s12265-023-10458-7

ORIGINAL ARTICLE

Upregulation of eIF2α by m^{6}A modification accelerates the proliferation of pulmonary artery smooth muscle cells in MCT-induced pulmonary arterial hypertension rats

Jing Zhang[1] · Wen-Qian Huang[1,2,3] · Yu-Rong Zhang[1] · Na Liang[4] · Nan-Ping Li[1,4] · Gang-Kai Tan[1,4] · Shao-Xin Gong[5] · Ai-Ping Wang[1,2]

Received: 28 June 2023 / Accepted: 30 October 2023 / Published online: 16 November 2023

Abstract

Pulmonary arterial hypertension (PAH) is a malignant cardiovascular disease. Eukaryotic initiation factor 2α (eIF2α) plays an important role in the proliferation of pulmonary artery smooth muscle cells (PASMCs) in hypoxia-induced pulmonary hypertension (HPH) rats. However, the regulatory mechanism of eIF2α remains poorly understood in PAH rats. Here, we discover eIF2α is markedly upregulated in monocrotaline (MCT)-induced PAH rats, eIF2α can be upregulated by mRNA methylation, and upregulated eIF2α can promote PASMC proliferation in MCT-PAH rats. GSK2606414, eIF2α inhibitor, can downregulate the expression of eIF2α and alleviate PASMC proliferation in MCT-PAH rats. And we further discover the mRNA of eIF2α has a common sequence with N 6-methyladenosine (m^{6}A) modification by bioinformatics analysis, and the expression of METTL3, WTAP, and YTHDF1 is upregulated in MCT-PAH rats. These findings suggest a potentially novel mechanism by which eIF2α is upregulated by m^{6}A modification in MCT-PAH rats, which is involved in the pathogenesis of PAH.

Keywords eIF2α · m^{6}A methylation · PASMCs · Pulmonary arterial hypertension · WTAP

Introduction

Pulmonary arterial hypertension (PAH) is a malignant cardiovascular disease and will eventually lead to right ventricular failure and even death, the mean survival is 2.8 years, and the rate of mortality in the first year is about 15% [1–3]. The underlying reason for the high mortality as well as the lack of effective therapeutic drugs and tools for PAH is that the physiopathologic mechanism is not fully understood in PAH [3]. Therefore, it is of great importance to further explore the new effective mechanism and potential target for intervention and treatment in PAH.

Studies have shown that the histologic features of PAH are complex and variable [3]. However, there are critical pathological features of the disorder that involve the uncontrolled growth of PASMCs [4]. Undoubtedly, PASMC proliferation is affected by many factors [4]. The eukaryotic initiation factor 2 alpha (eIF2α), also known as eukaryotic Initiation Factor 2 alpha, is an essential protein involved in the process of translation initiation in eukaryotic cells. eIF2α is part of the eIF2 complex, which is responsible for mediating the binding of initiator tRNA to the ribosome during translation initiation [5]. eIF2α is important in the regulation of protein

Associate Editor Nicola Smart oversaw the review of this article.

Jing Zhang and Wen-Qian Huang contributed equally to this work.

✉ Shao-Xin Gong
553648247@qq.com

✉ Ai-Ping Wang
waiping2011@163.com; waiping2011@usc.edu.cn

1 Department of Physiology, Institute of Neuroscience Research, Hengyang Medical School, University of South China, Hengyang 421001, Hunan, People's Republic of China

2 Institute of Clinical Research, Affiliated Nanhua Hospital, Hengyang Medical School, University of South China, Hengyang 421002, Hunan, People's Republic of China

3 Department of Blood Transfusion, the First Affiliated of Hainan Medical University, Haikou 570102, Hainan, People's Republic of China

4 Department of Anesthesiology, Affiliated Nanhua Hospital, Hengyang Medical School, University of South China, Hengyang 421002, Hunan, People's Republic of China

5 Department of Pathology, First Affiliated Hospital, Hengyang Medical School, University of South China, Hengyang 421001, Hunan, People's Republic of China

synthesis, and differential expression of eIF2α can cause cell proliferation in many human diseases [6]. Recent studies have shown that eIF2α plays a key role in the regulation of certain functional proteins to promote cell proliferation in tumor [5, 7]. Our team has found that eIF2α plays an important role in hypoxia-induced pulmonary hypertension (HPH) rats and monocrotaline (MCT)-induced PAH rats [8, 9]. However, its upstream regulatory mechanism has not been elucidated yet.

RNA from all living organisms can be post-transcriptionally modified by a collection of more than 100 distinct chemical modifications [10]. Among these modifications, N 6-methyladenosine (m^6A) modification has been identified as the most abundant internal modification in eukaryotic mRNA [11–14]. m^6A modification directs mRNAs to distinct fates such as cell differentiation, embryonic development, and stress responses [15]. In molecular mechanism, m^6A modification participates in almost all steps of mRNA metabolism, including mRNA translation, degradation, splicing, export, and folding [16]. In addition, m^6A modification is regulated by RNA methyltransferase (writers) that contain methyltransferase-like 3 (METTL3), methyltransferase-like 14 (METTL14), and Wilms tumor-associated protein (WTAP) in mammalian cells [17]. Three classes of m^6A readers have been characterized, based on how they bind to m^6A modified RNAs [18]. One major class is the YT521-B homology (YTH) domain family of proteins that directly bind to m^6A-modified sites (YTHDF1/2/3 and YTHDFC1/2) [19]. YTHDF1 has been identified as a translation-facilitating m^6A reader that recruits translation machinery to its target mRNAs in the cytoplasm [20]. The role of m^6A modification in cell proliferation has been reported recently [17, 21–23]. m^6A levels and the expression of methylation-related enzymes were altered in PAH rats, in which FTO and YTHDF1 may play a crucial role in m^6A modification [24]. m^6A modification-mediated GRAP regulates vascular remodeling in hypoxic pulmonary hypertension [25]. SEDT2/METTL14-mediated m^6A methylation awakening contributes to hypoxia-induced pulmonary arterial hypertension in mice [26]. Considering the crucial role of eIF2α in the proliferation of PASMCs in MCT-PAH rats, is the upstream regulatory mechanism of eIF2α related to m^6A modification? We further discovered that there are methylation modification sites on eIF2α mRNA by bioinformatics analysis. Therefore, we hypothesize that eIF2α plays a crucial role in the pathogenesis of MCT-PAH rats and that its upstream regulatory mechanism involves METTL3, WTAP, and YTHDF1-mediated m^6A modification.

Methods

Animals

Adult male Sprague–Dawley (SD) rats (weighing 150–200 g) were obtained from Hunan SJA Laboratory Animal Co., Ltd (Changsha, People's Republic of China). The experimental protocol was approved by the medicine animal welfare committee of Medicine School, University of South China (Hengyang, People's Republic of China); the animal protocol ethics number is 446.

Animals' Experiments

Adult male Sprague–Dawley (150–200 g in body weight) rats were randomly divided into control or MCT/vehicle rats. Experimental rats were administered an intraperitoneal injection of monocrotaline (60 mg/kg, Sigma, 315–22-0), and their littermates were injected with saline. For GSK2606414 treatment, rats that underwent monocrotaline treatment were treated either with vehicle or GSK2606414 (10 mg/kg, Sigma, 1,337,531–89-1) by intraperitoneal injection per day. GSK2606414 was dissolved in a mixture of dimethyl sulfoxide (DMSO): polyethylene glycol (PEG) 400: distilled water (1: 4: 5). After 4 weeks, RV systolic blood pressure (RVSP) was measured with pressure transducers under anesthesia. The RV hypertrophy was analyzed as a ratio of RV to left ventricular and septal weight. Left lung tissues were fixed in 4% paraformaldehyde solution for the following histology staining; right lung tissues and pulmonary arteries were excised and immediately frozen in liquid nitrogen for other experiments.

Assessment of PH

At the end of the experiment, the animals were anesthetized with ketamine (60 mg/kg IM) and xylazine (3 mg/kg IM), and right ventricle systolic pressure (RVSP) and mean pulmonary artery pressure (mPAP) were monitored. Briefly, a silicone catheter of outer diameter (0.9 mm, TIMON, Chengdu, China) was introduced into the pulmonary artery through the right vena jugularis externa, passing the right atrium and right ventricle in turn. A multichannel physiological recorder (BL-410, Chinese) was connected to the other end of the catheter to detect pressure. The position of the catheter tip was determined by the waveform during pressure measuring. It followed that we could confirm the pressure of RVSP and mPAP according to the waveform. Therefore, the right ventricular systolic pressure (RVSP) and mean pulmonary artery pressure (mPAP) were in turn recorded. After killing the animals, the right and left ventricle (RV, LV) and the interventricular septum (S) were dissected. The tibia length was measured and weighed for calculating the ratio of RV to (LV + S) and tibia length to RV, which are the key indexes used for evaluating RV hyperplasia. The freshly isolated pulmonary arterial samples were used for analysis of mRNA and protein expression. The left lung was fixed in 4% buffered

paraformaldehyde for 48 h and was used for hematoxylin and eosin (H&E) staining. The other part was snap-frozen in liquid nitrogen and stored at -80 °C for further assays.

HE Staining

The isolated rat lung tissue was stained with HE to assess the degree of pulmonary vascular remodeling. Lung tissue was removed and fixed in 4% paraformaldehyde solution for 24 h. Then, the tissues were subsequently dehydrated and embedded in paraffin and sliced into 4 μm cross-sections. The sections were stained with hematoxylin and eosin, and images were obtained using ZEISS LSM 880 Confocal Microscope (ZEISS, Jena, Germany).

Western Blot Analysis

Protease inhibitors (beyotime, Jiangsu, China) were used during the isolation process. Protein was extracted from pulmonary artery with RIPA (beyotime, Jiangsu, China) buffer (contains 0.1% PMSF). Protein concentration was determined using Enhanced BCA Protein Assay Kit (beyotime, Jiangsu, China). Equal amounts of protein from each sample (20 mg) were separated by 12% or 6% sodium dodecyl sulfate polyacrylamide gel electrophoresis and transferred to 0.45-mm polyvinylidine fluoride membranes (Millipore Corporation, Bedford, MA, USA). The membranes were blocked using 5% nonfat dry milk in tris-buffered saline containing 0.1% Tween-20 for 1 h, and then incubated with primary antibodies overnight at 4 °C. In the following day, the membranes were incubated for 1 h at 37 °C with horseradish horseradish peroxidase-coupled goat anti-rat secondary antibody (beyotime, A0208, 1:5000,) or peroxidase-coupled goat anti-mouse secondary antibody (beyotime, A0216, 1:5000,). The chemiluminescence signals were detected with the EasySee Western Blot Kit (Beijing TransGen Biotech, Beijing, China). The densitometric analysis was conducted with Image J 1.43 (National Institutes of Health). The following primary antibodies were used: Ki-67 (Abcam, ab92742, 1:2000), PCNA rabbit mAb (CST, 13,110, 1:1500), eIF2α (CST, 5324, 1:1500), WTAP (Abcam, ab195380, 1:2000), METTL3 (Proteintech, 67,733–1-Ig, 1:5000), YTHDF1 (Proteintech, 66,745–1-Ig, 1:1000), and β-Actin (BOSTER, BM3873,1:200).

Tissue Harvest, Sectioning, and Staining

All the left lung tissues were harvested and fixed at 4 ℃ overnight with fresh 4% paraformaldehyde (PFA). The tissues were then rinsed with PBS 4 times (5 min/each) and incubated in 30% sucrose in PBS at 4 ℃ overnight. Afterwards, the tissues are soaked in Tissue-Tek® O.C.T. Compound was then frozen at − 20 ℃ for cryosectioning at 6 μm thickness; cryosections were permeabilized with 0.1% Triton X-100 in PBS, blocked in 1% BSA for 30 min at room temperature, incubated with primary antibodies for 1 h at room temperature or overnight at 4 ℃, washed, incubated with appropriate secondary antibodies diluted in blocking buffer for 45 min at room temperature, washed, and counterstained with DAPI.

The following primary antibodies were used: Ki-67 (Abcam, ab92742, 1:200), eIF2α (CST, 5324, 1:100), and WTAP (Abcam, ab195380, 1:100).

All secondary antibodies were Alexa Fluor conjugates (488, 594) and used at 1:200 dilution (Life Technologies). Images were obtained using ZEISS LSM 880 Confocal Microscope (ZEISS, Jena, Germany). To measure fluorescent intensity in lung sections after immunofluorescence staining, three to six random fields of view (20 × objective) were captured with the same parameters across different groups. And three to six higher magnification images (40 × objective) focusing on individual pulmonary vessels were taken in each lung section. Fluorescent images were analyzed in a blinded manner. A threshold of "background" was calculated in images from a negative control slide stained by secondary antibody only or a nonfluorescent area of the same image. After eliminating the background in all images, cells were manually counted based on immunofluorescence staining of markers for each of the respective cell types [27–29].

Quantitative PCR (qPCR)

Total RNA was extracted from the pulmonary artery using Trizol (Invitrogen) and RNeasy Mini RNA extraction kit (Qiagen). RT-PCR was then performed to obtain the corresponding cDNA using iScript Select cDNA Synthesis Kit (Bio-Rad). qPCR was performed using SYBR Green (Bio-Rad) by CFX ConnectTM system (Bio-Rad). At least three technical and three biological replicates were performed for each protein if not otherwise notated. All primers are listed in Table 1.

Data Acquisition

The m^6A modification sites about eIF2α were obtained from RNA Modification Variant Database (RMVar) online database (http://www.rmvar.renlab.org/browse.html) and sequence-based RNA adenosine methylation site predictor (SRAMP) online website (http://www.cuilab.cn/sramp).

Statistical Analysis

The standard error was calculated from the average of at least three independent pulmonary artery samples unless otherwise mentioned. All results were presented as the

Table 1 qPCR primer list

Gene name	Sequence
eIF2α	5′-GGACAAATGGAAGTATGGGATG -3′ 5′-CAAGAGAGAGCCAGTGTAATGC -3′
β-actin	5′-CCCATCTATGAGGGTTACGC-3′ 5′-TTTAATGTCACGCACGATTTC-3′

mean ± standard error of the mean (SEM). Statistical analysis of the differences between groups was performed by GraphPad Prism 5.0 and SPSS 19.0 software using one-way ANOVA. $P < 0.05$ was considered significant. The experimental data was analyzed without any pre-set bias, and no particular criteria to exclude or include any specific sample from the analysis was used.

Results

Vascular Remodeling and eIF2α Markedly Increased in MCT-Induced PAH Rats

To clarify whether the establishment of the MCT-PAH rats was successful, we analyzed hemodynamic data in SD rats. In MCT-PAH rats, the weight of rats was downgraded (Fig. 1a); right ventricular systolic pressure (RVSP), mean pulmonary arterial pressure (mPAP), RV/(LV + S) (the ratio of right ventricle to (left ventricle + septum)), and the ratio of right ventricular/tibia length were significantly increased compared with that in control rats (Fig. 1b–e). These data suggest that the establishment of the MCT-PAH rats was successful.

The pulmonary arteries showed significant thickening, and the percentage of the medial thickness of the pulmonary arterioles (WT%) was significantly increased in MCT-PAH rats compared with that in control rats by HE staining (Fig. 1f). The protein expression of PCNA in MCT-PAH rats increased in pulmonary artery tissues compared with that in control rats by Western blot (Fig. 1g). Furthermore, the protein expression of Ki-67 in MCT-PAH rats increased in PASMCs compared with that in control rats by immunofluorescence (Fig. 1h, i). These data suggest that vascular remodeling was obviously increased in MCT-PAH rats.

Interestingly, the expression of eIF2α mRNA was upregulated in pulmonary artery tissues in MCT-PAH rats compared with that in control rats (Fig. 2a). The expression of eIF2α exhibited an increase in pulmonary artery tissues by Western blot and in PASMCs by immunofluorescence in MCT-PAH rats compared with that in control rats (Fig. 2b–d). These results strongly support that eIF2α plays an important role in the development of MCT-PAH rats.

GSK2606414, eIF2α Inhibitor, Can Significantly Downregulate the Expression of eIF2α in MCT-Induced PAH Rats

To further explore the role of eIF2α in pulmonary vascular remodeling in MCT-PAH rats, we used GSK2606414, eIF2α inhibitor, which is a novel and highly selective inhibitor of protein kinase R-like endoplasmic reticulum kinase (PERK). We found the expression of eIF2α was observably downregulated in GSK2606414-treated PAH rats in pulmonary artery tissues by Western blot and in PASMCs by immunofluorescence compared with that in MCT-PAH rats (Fig. 3a–c). These results strongly support that GSK2606414 can significantly downregulated the expression of eIF2α in MCT-PAH rats.

GSK2606414, eIF2α Inhibitor, Can Alleviate Vascular Remodeling in MCT-Induced PAH Rats

In GSK2606414-treated PAH rats, mPAP, RVSP, the ratios of RV/LV + S, and RV/tibial length were evidently downregulated compared with that in MCT-PAH rats (Fig. 4a–d). These data suggest that targeting inhibition of eIF2α could attenuate the progression of MCT-induced PAH rats.

The WT% was significantly decreased in the GSK2606414-treated rats compared with that in MCT rats by HE staining (Fig. 4e). GSK2606414 evidently downregulated the protein expression of PCNA in pulmonary artery tissues compared with that in MCT-PAH rats by Western blot (Fig. 4f). And we found that GSK2606414 evidently downregulated the protein expression of Ki-67 in PASMCs compared with that in MCT-PAH rats by immunofluorescence (Fig. 4g, h). These data suggest that targeting inhibition of eIF2α can markedly alleviate PASMC proliferation and vascular remodeling in MCT-PAH rats.

The mRNA of eIF2α has a Common Sequence with m^{6}A Modification

Next, we sought to reveal the upstream mechanism of eIF2α in MCT-PAH rats. m^{6}A modification is the most abundant internal modification in eukaryotic mRNA, recent studies have found that m^{6}A modification could regulate pulmonary vascular remodeling in MCT-induced PAH rats [25]. Importantly, we found that the mRNA of eIF2α had a common sequence with m^{6}A modification by bioinformatic analysis (Fig. 5a, b). The results support that m^{6}A modification may be the upstream mechanism of eIF2α in MCT-PAH rats.

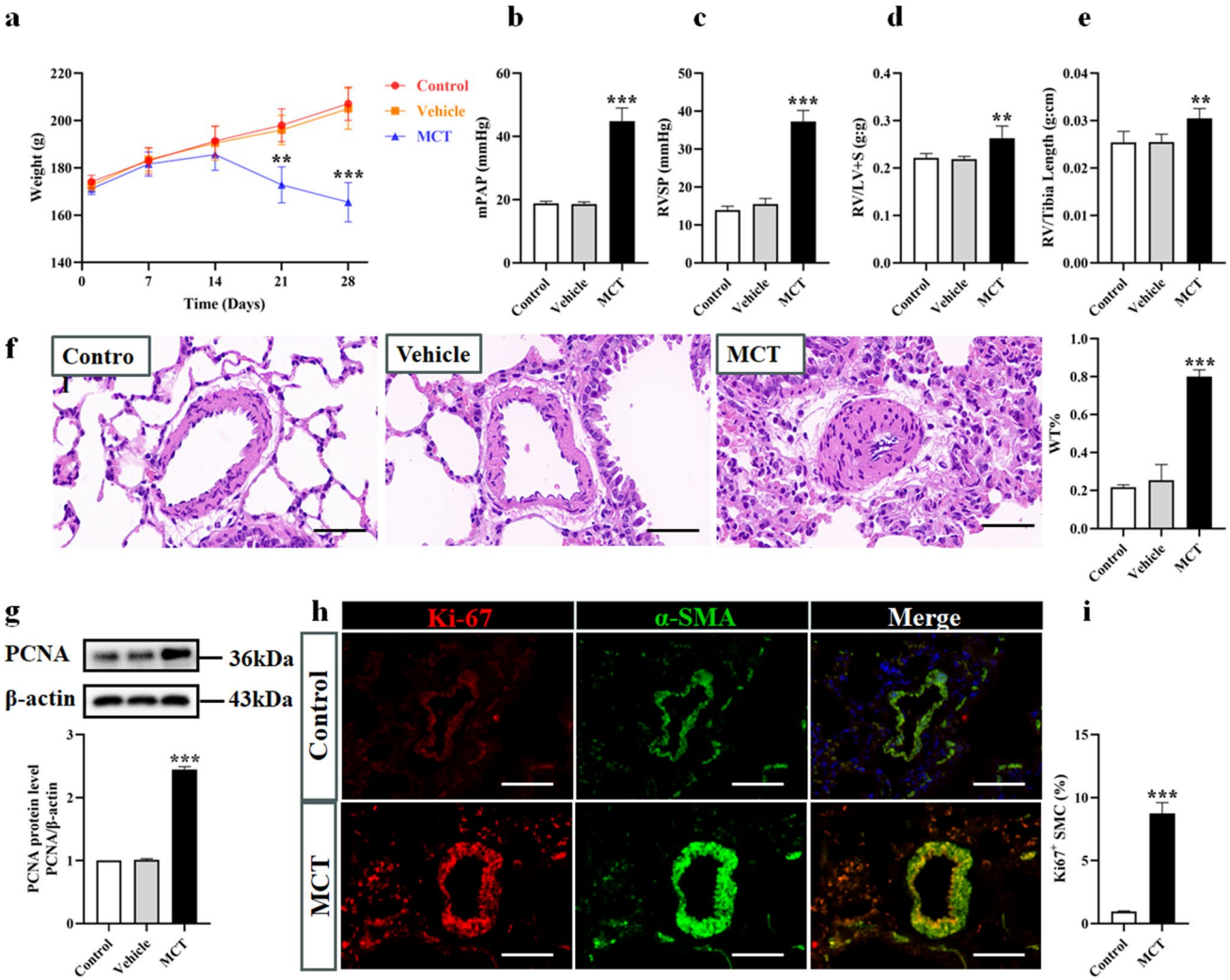

Fig. 1 Vascular remodeling in MCT-induced PAH rats. Rats were treated with MCT or vehicle. **a** Weight. **b** Mean pulmonary arterial pressure (mPAP). **c** Right ventricular systolic pressure (RVSP). **d** RV to left ventricular and septal weight (RV/LV + S). **e** RV/tibia length. **f** Representative hematoxylin and eosin-stained sections of small PAs and arterioles. Scale bars = 200 μm. **g** Immunoblotting of PCNA expressions in pulmonary artery tissue. **h**, **i** Representative immunofluorescence staining of lung tissue for Ki-67 (red) and α-SMA (α-smooth muscle actin) (green) in groups of rats. Nuclei are stained with 4′,6-diamidino-2-phenylindole (DAPI). Scale bar = 200 μm. Two-way ANOVA (Šidák's multiple-comparisons test) in **a**; one-way ANOVA (Dunnett *t*-test) in **b**–**g**; Student's *t*-test in *i*. $^{**}P < 0.01$, $^{***}P < 0.001$; error bars, mean ± SEM. $n = 6$

The Expression of METT3, YTHDF1, and WTAP are Dramatically Upregulated in MCT-Induced PAH Rats

Since the mRNA of eIF2α had a common sequence with m^{6}A modification by bioinformatic analysis, and recent studies have found that m^{6}A-related regulatory proteins are newly identified as important targets for regulating cell proliferation [17, 21–23], nextly, we detected the expression of m^{6}A-related regulatory proteins in MCT-PAH rats. We found that METTL3, WTAP, and YTHDF1 expression were significantly upregulated in pulmonary artery tissues in MCT-PAH rats compared with that in control rats by Western blot (Fig. 6 a–c). And the expression of WTAP was remarkably upregulated in PASMCs in MCT-PAH rats compared with that in control rats by immunofluorescence staining (Fig. 6 d, e). These results suggest that m^{6}A-related regulatory proteins may play an important role in MCT-PAH rats; importantly, eIF2α can be regulated by mRNA methylation (m^{6}A modification) in MCT-PAH rats.

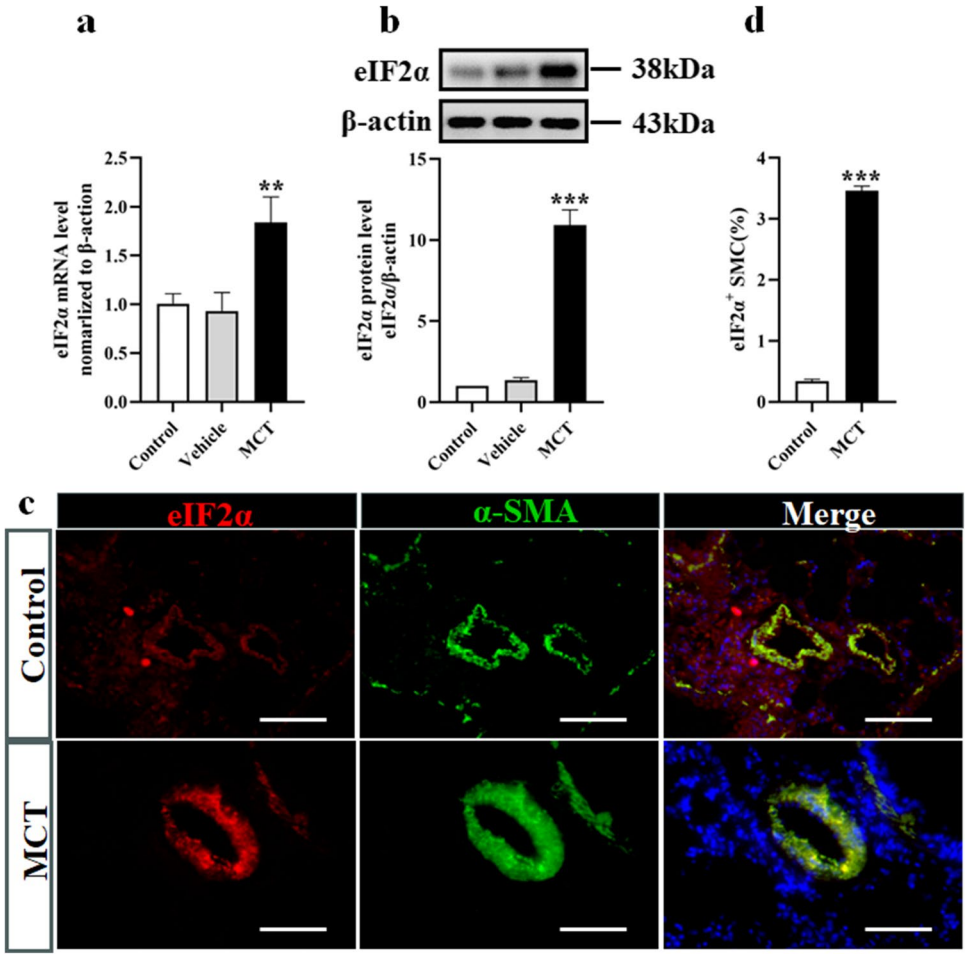

Fig. 2 eIF2α markedly increased in MCT-induced PAH rats. Rats were treated with MCT or vehicle. **a** qPCR analysis on the eIf2α genes in the pulmonary artery tissue of rats. **b** Immunoblotting of PCNA expressions in pulmonary artery tissue. **c**, **d** Representative immunofluorescence staining of lung tissue for eIf2α (red) and α-SMA (α-smooth muscle actin) (green) in groups of rats. Nuclei are stained with DAPI. Scale bar = 200 μm. One-way ANOVA (Dunnett *t*-test) in **a**, **b**; Student's *t*-test in **d**. $^{**}P < 0.01$, $^{***}P < 0.001$; error bars, mean ± SEM. $n = 6$

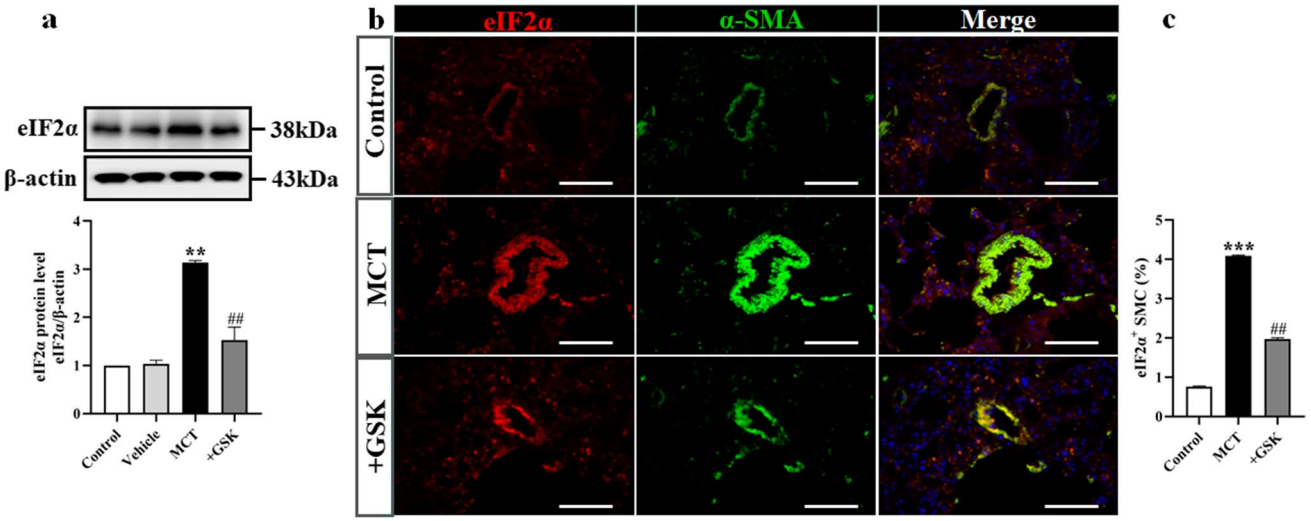

Fig. 3 GSK2606414, eIF2α inhibitor, can significantly downregulated the expression of eIF2α in MCT-induced PAH rats. Rats were treated with GSK2606414 or MCT. **a** Immunoblotting of PCNA expressions in pulmonary artery tissue. **b**, **c** Representative immunofluorescence staining of lung tissue for eIf2α (red) and α-SMA (α-smooth muscle actin) (green) in groups of rats. Nuclei are stained with DAPI. Scale bar = 200 μm. One-way ANOVA (Sidak test) in **a**, **c**. $^{**}P < 0.01$, $^{***}P < 0.001$, $^{\#\#}P < 0.01$; error bars, mean ± SEM. $n = 6$

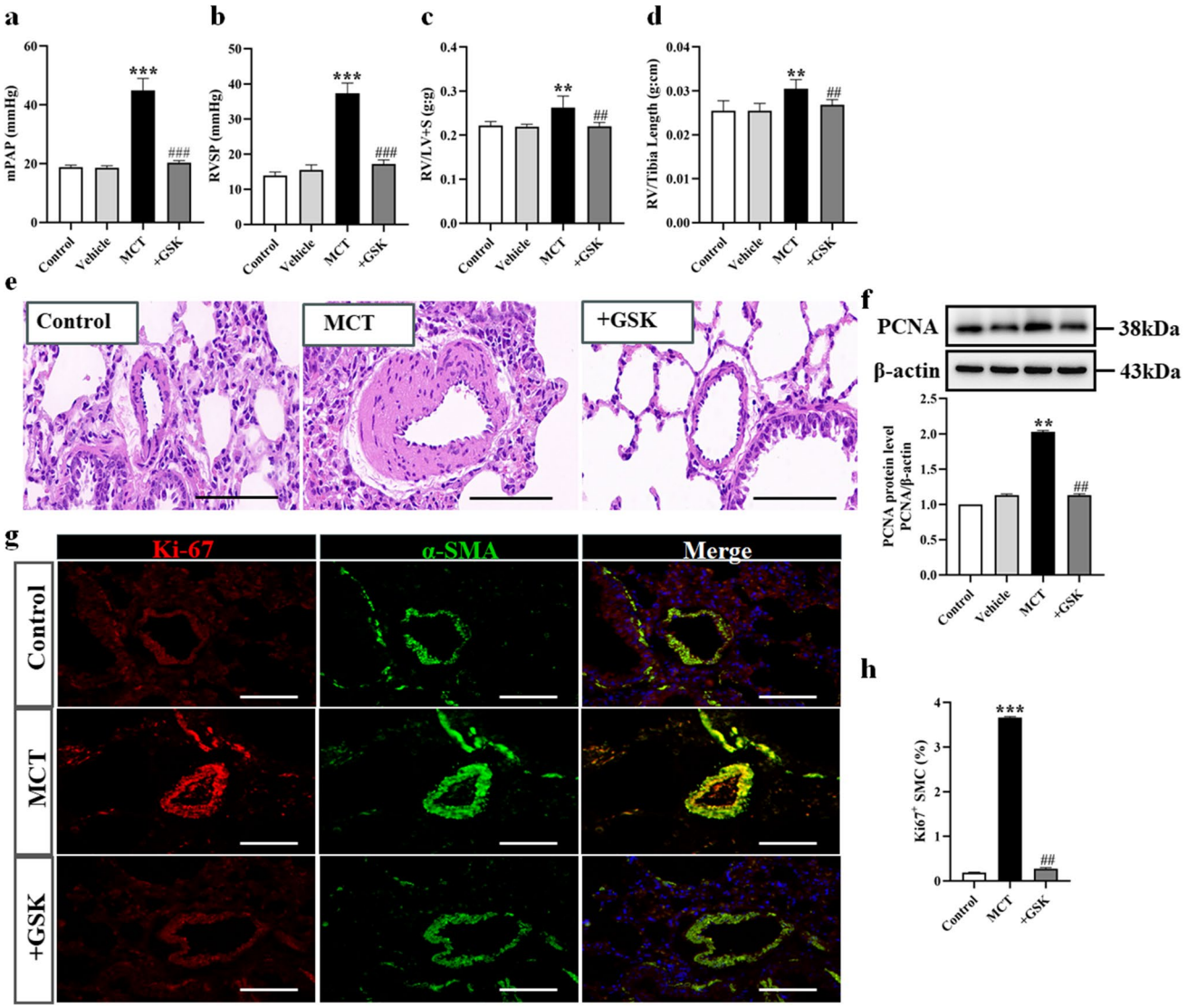

Fig. 4 eIF2α inhibitor can alleviate vascular remodeling in MCT-induced PAH rats. Rats were treated with GSK2606414 or MCT. **a** mPAP. **b** RVSP. **c** RV/LV + S. **d** RV/tibia length. **e** Representative hematoxylin and eosin-stained sections of small PAs and arterioles. Scale bars = 200 μm. **f** Immunoblotting of PCNA expressions in pulmonary artery tissue. **g**, **h** Representative immunofluorescence staining of lung tissue for Ki-67 (red) and α-SMA (α-smooth muscle actin) (green) in groups of rats. Nuclei are stained with DAPI. Scale bar = 200 μm. One-way ANOVA (Sidak test) in **a**–**d**, **f**, **h**. $^{**}P < 0.01$, $^{***}P < 0.001$, $^{\#\#}P < 0.01$, $^{\#\#\#}P < 0.001$; error bars, mean ± SEM. $n = 6$

Discussion

PAH is a disorder characterized by marked remodeling of the pulmonary vasculature and a progressive rise in the pulmonary vascular load, leading to hypertrophy and remodeling of the right ventricle [1]. Previous studies have shown that pulmonary vascular remodeling is the most important physiopathologic mechanism of PAH, and that the abnormal proliferation, hypertrophy, and secretion of PASMCs play an important role in PAH [3]. eIF2α, as a regulatory subunit of eIF2, is a key player of translation initiation factor [5]. Our previous studies have demonstrated that the expression of eIF2α is markedly upregulated in MCT-PAH rats and HPH rats, and the above two effects can be inhibited by eIF2α siRNA. But the upstream regulatory mechanism of eIF2α has not been elucidated in PAH rats. Based on the above research, we established the model of MCT-PAH rats. Firstly, we discover eIF2α is upregulated in MCT-PAH rats. Additionally, downregulation of the expression of eIF2α by using GSK2606414 could alleviate PASMC proliferation and pulmonary vascular remodeling in MCT-PAH. Then, we further discover the mRNA of eIF2α has a common sequence with m^6A modification by bioinformatics analysis, further research found that METTL3, WTAP, and YTHDF1 are significantly upregulated in MCT-PAH rats. These results suggest that eIF2α may play an important role

a

#	Position	Sequence context	Structural context	Local structure visualization	Score(binary)	Score(knn)	Score(spectrum)	Score(combined)	Decision
1	107	ATTTT TTGGC CATAG ACCAC AGACT TTAAC ATGGC CCTGA CGTCG	N/A	N/A	0.648	0.777	0.580	0.627	m^{6}A site (**High** confidence)
2	511	GCTGG AAGAT CTCTA CCAGA AGACC GCCTG GCACT TCGAG AAGAA	N/A	N/A	0.431	0.753	0.733	0.568	m^{6}A site (**Moderate** confidence)
3	689	CCCAC TGTCA AGATC CGTGC GGACA TCGAG TGCTC CTGCT ACGGT	N/A	N/A	0.595	0.81	0.639	0.623	m^{6}A site (**High** confidence)
4	841	GACCA CATCC ACTAC CAAGA AGACA GACGG TTTAA AGGCT CTGGA	N/A	N/A	0.478	0.679	0.719	0.584	m^{6}A site (**Moderate** confidence)
5	892	CATTG AGCAC ATTCG CGCCA AGACC AGCGA GTACG ATGGA GAGTT	N/A	N/A	0.410	0.319	0.722	0.530	m^{6}A site (**Low** confidence)
6	936	TCAAG GTGAT CATGG CACCC AAACT GGTTA CGGCC ATCGA CGAGG	N/A	N/A	0.496	0.628	0.685	0.578	m^{6}A site (**Moderate** confidence)

b

Modification Type	Chromosome Position	Source	Species	Gene	Variant(s)	SNP Position	Database
m6A	chr2:37126323(-)	MeRIP-seq (Medium)	Human	EIF2AK2	rs759284406	chr2:37126317..37126321	dbSNP153
m6A	chr2:37126323(-)	MeRIP-seq (Medium)	Human	EIF2AK2	rs1340314941	chr2:37126324..37126324	dbSNP153
m6A	chr3:150552390(+)	miCLIP (High)	Human	EIF2A	rs1489128272	chr3:150552391..150552391	dbSNP153
m6A	chr3:150562572(+)	DART-seq (High)	Human	EIF2A	rs1193126169	chr3:150562573..150562573	dbSNP153
m6A	chr3:150562580(+)	DART-seq (High)	Human	EIF2A	rs774888051	chr3:150562580..150562580	dbSNP153
m6A	chr3:150572053(+)	miCLIP (High)	Human	EIF2A	rs1243376359	chr3:150572053..150572053	dbSNP153
m6A	chr3:150572124(+)	m6A-REF-seq&miCLIP (High)	Human	EIF2A	rs573613349	chr3:150572124..150572124	dbSNP153
m6A	chr3:150572163(+)	DART-seq&m6A-REF-seq&miCLIP (High)	Human	EIF2A	rs1244450729	chr3:150572165..150572165	dbSNP153
m6A	chr3:150572208(+)	miCLIP (High)	Human	EIF2A	rs1320527387	chr3:150572208..150572209	dbSNP153
m6A	chr3:150572419(+)	miCLIP (High)	Human	EIF2A	rs1334437510	chr3:150572420..150572420	dbSNP153

Fig. 5 The mRNA of eIF2α has a common sequence with m^{6}A modification. **a** Bioinformatic analysis of SRAMP websites showed that the mRNA of eIF2α had a common sequence with m^{6}A modification. **b** Bioinformatic analysis of RMVar websites showed that the mRNA of eIF2α had a common sequence with m^{6}A modification

in promoting PASMC proliferation in MCT-PAH rats, that its upstream regulatory mechanism can involve METTL3, WTAP, and YTHDF1-mediated m^{6}A modification.

We have confirmed that eIF2α plays an important role in pulmonary vascular remodeling, but the upstream regulation mechanism has not been elucidated. m^{6}A modification is the most prevalent internal modification existing on eukaryotic mRNA, and it impacts a variety of physiological events [11]. As an epigenetics, m^{6}A modification has been shown to play an important role in cardiovascular diseases in recent years [23, 30]. Both METTL3 and WTAP, as m^{6}A-modified methyltransferase, and YTHDF1, as m^{6}A-modified reading protein, play important roles in a variety of cardiovascular diseases [19, 31–33]. Recent studies have shown that m^{6}A-modified regulatory proteins, such as METTL3, WTAP, and YTHDF1, are crucial in regulating cell proliferation [34, 35]. METTL3 facilitates glycolysis and cardiac fibroblast proliferation, leading to cardiac fibrosis [36]. WTAP could promote the proliferation of mTORC1-activated cancer cells [30]. YTHDF1 regulates cardiomyocyte proliferation and heart regeneration by demethylating the mRNA [34]. Thus, we reasoned that the proliferation of PASMCs in MCT-induced PAH rats might also be regulated by the upregulation of eIF2α by METTL3, WTAP, and YTHDF1-mediated m^{6}A modification.

Based on the critical role of eIF2α in MCT-induced PAH rats and on the basis that m^{6}A modification can

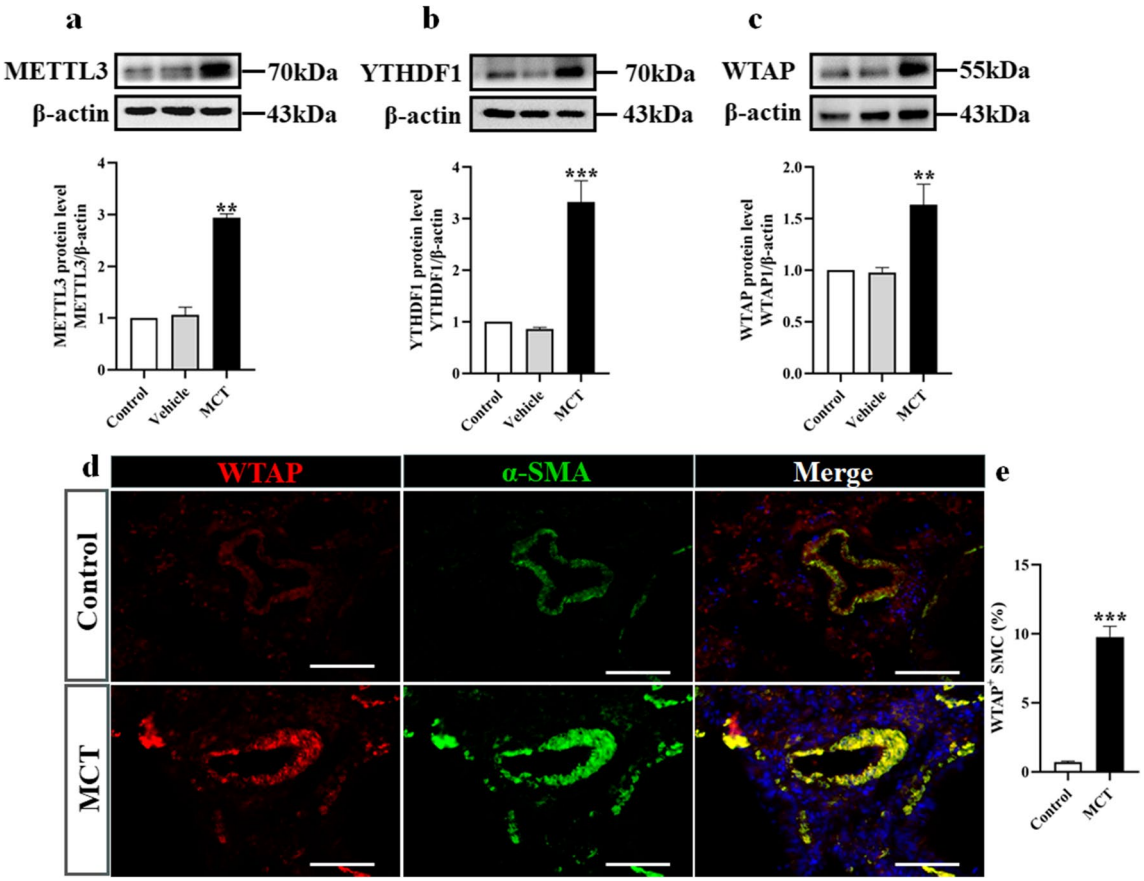

Fig. 6 The expression of METT3, YTHDF1, and WTAP are dramatically upregulated in MCT-induced PAH rats. Rats were treated with MCT or vehicle. **a** Immunoblotting of METTL3 expressions in pulmonary artery tissue. **b** Immunoblotting of YTHDF1 expressions in pulmonary artery tissue. **c** Immunoblotting of WTAP expressions in pulmonary artery tissue. **d**, **e** Representative immunofluorescence staining of lung tissue for WTAP (red) and α-SMA (α-smooth muscle actin) (green) in groups of rats. Nuclei are stained with DAPI. Scale bar = 200 μm. One-way ANOVA (Dunnett *t*-test) in **a**–**c**; Student's *t*-test in **e**. $^{**}P < 0.01$, $^{***}P < 0.001$; error bars, mean ± SEM. $n = 6$

modulate pulmonary vascular remodeling in PAH, we use SRAMP and RMVAR database to make m^{6}A locus prediction, further, to confirm our hypothesis. First, SRAMP result showed that there was a high-confidence m^{6}A site on eIF2α mRNA. Second, the RMVAR database also showed that, based on the results of m^{6}A-REF-seq and MICILP data sequencing, multiple sites of high confidence for m^{6}A were present on the mRNA of eIF2α, particularly possibly regulated by YTHDF1. These results suggest that eIF2α mRNA have multiple sites of m^{6}A modification, upregulated of eIF2α by m^{6}A modification can accelerate the proliferation of PASMCs in MCT-PAH rats. And then we find that the expression of METT3, YTHDF1, and WTAP are dramatically upregulated in MCT-PAH rats; these results suggest that m^{6}A modification is involved in MCT-PAH rats. The limitation of this study is that we lack direct evidence to directly demonstrate a clear relationship between m6A modification and eIF2α expression, and the individual contributions of METT3, YTHDF1, and WTAP to PAH development were not further investigated. And although PAH rat model partly captured key characteristics of PAH patients, there are remaining human patients features that cannot be reliably detected and rigorously investigated in rats; documented physiological differences between human and rats should be taken into consideration when interpreting physiological data from rats. Collectively, these data further supported that the pivotal and novel pathogenic role of eIF2α in MCT-PAH rats, and its upstream regulatory mechanism can involve METTL3, WTAP, and YTHDF1-mediated m^{6}A modification, which suggests that upregulation of eIF2α by METTL3, WTAP, and YTHDF1-mediated m^{6}A modification can be a potential target in PAH.

PAH is a rare but lethal disease. Increased pulmonary vascular resistance in PAH is driven by vasoconstriction, inflammation, and proliferative remodeling of the intima and media of precapillary arteries. This study provides new insight that upregulation of eIF2α by METTL3, WTAP, and YTHDF1-mediated m^{6}A modification can be a key physiopathologic mechanism in pulmonary vascular remodeling in PAH rats. In

particular, we discuss the vital role of eIF2α in MCT-PAH rats. GSK2606414, eIF2α inhibitor, can alleviate PASMCS proliferation and pulmonary vascular remodeling in MCT-PAH rats. Furthermore, we discuss the new regulatory pathway of eIF2α in PASMCs proliferation and pulmonary vascular remodeling by METTL3, WTAP, and YTHDF1-mediated m^6A modification pathway. These results emphasize the important role played by eIF2α in MCT-PAH rats; the upregulation of eIF2α by METTL3, WTAP, and YTHDF1-mediated m^6A modification can be a new regulatory pathway in MCT-PAH rats.

Funding This project was supported by the National Natural Science Foundation of China (grant number 81600040 to Wang AP), and the Natural Science Foundation of the Province of Hunan (grant number 2021JJ30601 to Wang AP), Key Program of Education Department of Hunan Province (grant number 21A0274 to Wang AP), Research project of Health Commission of Hunan Province (grant number 202204114218 to Liang N).

Declarations

Human Research Statement No human studies were carried out by the authors for this article.

Animal Research Statement All institutional and national guidelines for the care and use of laboratory animals were followed and approved by the appropriate institutional committees.

Conflict of Interest The authors declare no competing interests.

References

1. Poch D, Mandel J. Pulmonary hypertension. Ann Intern Med. 2021;174(4):ITC49–64.
2. Burki TK. Pharmacotherapy for pulmonary arterial hypertension. Lancet Respir Med. 2020;8(11): e81.
3. Parikh V, Bhardwaj A, Nair A. Pharmacotherapy for pulmonary arterial hypertension. J Thorac Dis. 2019;11(Suppl 14):S1767–81.
4. Hassoun PM. Pulmonary arterial hypertension. N Engl J Med. 2021;385(25):2361–76.
5. Baird TD, Wek RC. Eukaryotic initiation factor 2 phosphorylation and translational control in metabolism. Adv Nutr. 2012;3(3):307–21.
6. Donnelly N, Gorman AM, Gupta S, et al. The eIF2alpha kinases: their structures and functions. Cell Mol Life Sci. 2013;70(19):3493–511.
7. Zheng Q, Ye J, Cao J. Translational regulator eIF2alpha in tumor. Tumour Biol. 2014;35(7):6255–64.
8. Guo L, Li Y, Tian Y, et al. eIF2alpha promotes vascular remodeling via autophagy in monocrotaline-induced pulmonary arterial hypertension rats. Drug Des Devel Ther. 2019;13:2799–809.
9. Wang AP, Li XH, Yang YM, et al. A critical role of the mTOR/eIF2alpha pathway in hypoxia-induced pulmonary hypertension. PLoS One. 2015;10(6): e0130806.
10 Machnicka MA, Milanowska K, Osman Oglou O, et al. MODOMICS: a database of RNA modification pathways–2013 update. Nucleic Acids Res. 2013;41(Database issue):262–7.
11. Desrosiers R, Friderici K, Rottman F. Identification of methylated nucleosides in messenger RNA from Novikoff hepatoma cells. Proc Natl Acad Sci U S A. 1974;71(10):3971–5.
12. Furuichi Y, Morgan M, Shatkin AJ, et al. Methylated, blocked 5 termini in HeLa cell mRNA. Proc Natl Acad Sci U S A. 1975;72(5):1904–8.
13. Lavi S, Shatkin AJ. Methylated simian virus 40-specific RNA from nuclei and cytoplasm of infected BSC-1 cells. Proc Natl Acad Sci U S A. 1975;72(6):2012–6.
14. Adams JM, Cory S. Modified nucleosides and bizarre 5′-termini in mouse myeloma mRNA. Nature. 1975;255(5503):28–33.
15. Zhao BS, Roundtree IA, He C. Post-transcriptional gene regulation by mRNA modifications. Nat Rev Mol Cell Biol. 2017;18(1):31–42.
16. Fu Y, Dominissini D, Rechavi G, et al. Gene expression regulation mediated through reversible m(6)A RNA methylation. Nat Rev Genet. 2014;15(5):293–306.
17. Huang J, Sun W, Wang Z, et al. FTO suppresses glycolysis and growth of papillary thyroid cancer via decreasing stability of APOE mRNA in an N6-methyladenosine-dependent manner. J Exp Clin Cancer Res. 2022;41(1):42.
18. Raudvere U, Kolberg L, Kuzmin I, et al. g:Profiler: a web server for functional enrichment analysis and conversions of gene lists (2019 update). Nucleic Acids Res. 2019;47(W1):W191–8.
19. Wang X, Zhao BS, Roundtree IA, et al. N(6)-methyladenosine modulates messenger RNA translation efficiency. Cell. 2015;161(6):1388–99.
20. Yu G, Wang LG, Han Y, et al. clusterProfiler: an R package for comparing biological themes among gene clusters. OMICS. 2012;16(5):284–7.
21. Du A, Li S, Zhou Y, et al. M6A-mediated upregulation of circMDK promotes tumorigenesis and acts as a nanotherapeutic target in hepatocellular carcinoma. Mol Cancer. 2022;21(1):109.
22. Yang Z, Wang T, Wu D, et al. RNA N6-methyladenosine reader IGF2BP3 regulates cell cycle and angiogenesis in colon cancer. J Exp Clin Cancer Res. 2020;39(1):203.
23. Yin H, Zhang X, Yang P, et al. RNA m6A methylation orchestrates cancer growth and metastasis via macrophage reprogramming. Nat Commun. 2021;12(1):1394.
24. Zeng Y, Huang T, Zuo W, et al. Integrated analysis of m(6)A mRNA methylation in rats with monocrotaline-induced pulmonary arterial hypertension. Aging (Albany NY). 2021;13(14):18238–56.
25. Liu P, Zhang A, Ding Z, et al. m(6)A Modification-mediated GRAP regulates vascular remodeling in hypoxic pulmonary hypertension. Am J Respir Cell Mol Biol. 2022;67(5):574–88.
26. Zhou XL, Huang FJ, Li Y, et al. SEDT2/METTL14-mediated m6A methylation awakening contributes to hypoxia-induced pulmonary arterial hypertension in mice. Aging (Albany NY). 2021;13(5):7538–48.
27 Shihan MH, Novo SG, Le Marchand SJ, et al. A simple method for quantitating confocal fluorescent images. Biochem Biophys Rep. 2021;25(2405-5808 (Electronic)):100916.
28. Zhou W, Liu K, Zeng L, et al. Targeting VEGF-A/VEGFR2 Y949 signaling-mediated vascular permeability alleviates hypoxic pulmonary hypertension. Circulation. 2022;146(24):1855–81.
29. Shivaraju M, Chitta UK, Grange RMH, et al. Airway stem cells sense hypoxia and differentiate into protective solitary neuroendocrine cells. Science. 2021;371(6524):52–7.
30. Wu S, Zhang S, Wu X, et al. m(6)A RNA methylation in cardiovascular diseases. Mol Ther. 2020;28(10):2111–9.
31. Ping XL, Sun BF, Wang L, et al. Mammalian WTAP is a regulatory subunit of the RNA N6-methyladenosine methyltransferase. Cell Res. 2014;24(2):177–89.

32. Yang X, Zhang S, He C, et al. METTL14 suppresses proliferation and metastasis of colorectal cancer by down-regulating oncogenic long non-coding RNA XIST. Mol Cancer. 2020;19(1):46.
33. Hu L, Wang J, Huang H, et al. YTHDF1 regulates pulmonary hypertension through translational control of MAGED1. Am J Respir Crit Care Med. 2021;203(9):1158–72.
34. Han Z, Wang X, Xu Z, et al. ALKBH5 regulates cardiomyocyte proliferation and heart regeneration by demethylating the mRNA of YTHDF1. Theranostics. 2021;11(6):3000–16.
35. Dorn LE, Lasman L, Chen J, et al. The N(6)-Methyladenosine mRNA methylase METTL3 controls cardiac homeostasis and hypertrophy. Circulation. 2019;139(4):533–45.
36. Zhou Y, Song K, Tu B, et al. METTL3 boosts glycolysis and cardiac fibroblast proliferation by increasing AR methylation. Int J Biol Macromol. 2022;223(Pt A):899–915.